

# High Speed Railway Bolt Detection Based on Deep Learning

Xiangyi Qin<sup>1,a</sup>

<sup>1</sup>School of Traffic and Transportation, Beijing Jiaotong University, Beijing, China

<sup>a</sup>xiangyiq0803@163.com

**Keywords:** Deep learning; Bolt defect detection; Adversarial generative network

**Abstract:** With the development of railway network, the safety maintenance and guarantee of transportation infrastructure is becoming more and more important. Under the high frequency vibration of train running, the bolt is easy to produce defects. At present, railway works departments collect track structure images by means of comprehensive inspection vehicles and manual trolley, but they rely on manual playback to find structural defects due to their limited ability of automatic identification of defects. Considering the Similarity of the inner and outer defective-free bolts of each rail platform, this work proposed a fast location algorithm of bolts based on Structural Similarity (SSIM). The Bidirectional Generative Adversarial Network (BiGAN) is selected and trained to identify the defect bolts, and is applied to 4.25 GB images of 25 km lines. The results show that the method can effectively identify the defective bolts, the recall rates of missing bolt and stampeding plate are 98.62% and 97.93% respectively, the recall rate of defective samples is 93.45%, the accuracy rate is 94.20%, and the misjudgment rate of normal samples is 5.13%.

## 1. Introduction

The defect of bolts will reduce the transverse stability of track, and the continuous multiple defective bolts may lead to the derailment of train, seriously affecting the operation safety of high-speed railway. In view of the structure of high-speed railway track, this work designs track defect identification technology for WJ-8B bolts. The original railway images are taken by line scan camera mounted under railway diagnostic trains and hand pushed inspection vehicle. Finding bolt defects by computer is by processing these railway images, first locate and segment the bolt subgraphs, and then identify each subgraph to tell whether it's a defect one or a defect-free.

For bolt defect identification, the present methods mostly adopt supervised or semi-supervised framework. That is to extract the features of the detected object, and then rely on the defect sample database to detect. The key is to build a high-quality feature encoder and to construct a full defect sample database. Dai Peng [4] used unsupervised sparse auto-coding network to extract spatial features of bolts, and then classified the samples of normal bolts and defective bolts through softmax layer. Min Yongzhi [5] used Canny operator to extract edges, and then classified edge features through template matching algorithm.

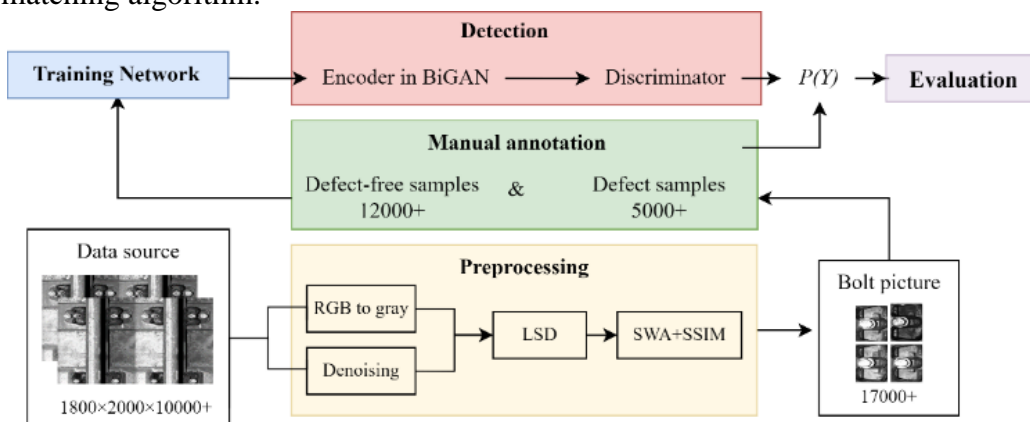


Figure 1: The overall work.

This work proposes a bolt localization algorithm based on structural similarity and a bolt defect recognition algorithm based on Bidirectional Generative Adversarial Network (BiGAN). Firstly, the Railway Surface Detection (RSD) algorithm and ASW (Adjusted Sliding Window) algorithm are used to locate the bolt and obtain the bolt subgraph. Then we train the BiGAN network by normal samples. By doing this, the encoder of the network can well extract feature, thus avoiding the pain point of constructing the full-defect bolt. The overall process of this work is shown in Figure 1.

## 2. Railway Image Acquisition

A railway video is acquired using DALSA Spyder2 line scan camera mounted under a diagnostic train. Each image in the video is  $1800 \times 2000$ . Figure 2 shows an example image.

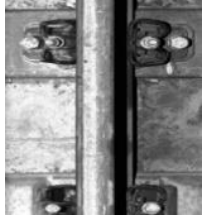


Figure 2: Railway example image.

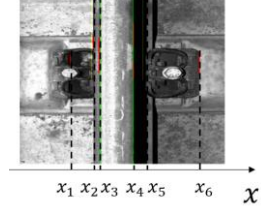


Figure 3: Line segments using LSD.

## 3. Bolt Subgraph Extraction

Bolt subgraph extraction is to locating the position of the bolt in the track image and extract the bolt subgraph. We can see in Figure 2 that the railway pictures have three prior information.

- The boundary of the rail surface is vertical to x-axis.
- The size of the same type of bolt is equal, and the longitudinal distance between adjacent bolt is fixed.
- Each frame of track image contains only one rail, and continuous track images can be connected to form a complete rail image.

Based on the above prior information, the process of extracting the bolt subgraph is constructed: firstly, each frame of track image is connected to form a section of rail, and the rail boundary position is determined based on Rail Surface Detection (LSD) Algorithm [8], and the range of the bolt to be selected is reduced from the whole image to the rail periphery. On this basis, the Sliding Window Algorithm (SWA) is used to extract the subgraph in the selected region, and the Structural Similarity (SSIM) between the extracted subgraph and the template bolt is calculated. The subgraph with the highest similarity result is the exact bolt subgraph.

### 3.1 RSD (Rail Surface Detection) Algorithm

Linear segment detector LSD is a fast linear segment detector that can extract linear segments in a certain range of directions in the picture, as shown in The red line segment in Figure 4. The rail edge segment has good continuity, so the rail boundary position can be located based on formula (1).

$$\arg \max_{r,l} \frac{TL(r)/LN(r)+TL(l)/LN(l)}{\sigma^2([l,r])} \quad (1)$$

Where  $TL(\cdot)$  represents the total length of segments perpendicular to y axis pixel,  $TN(\cdot)$  represents the total number of segments perpendicular to y axis pixel.  $(r-l) \in (0.9W, 1.1W)$  and  $r, l \in (l_m, r_m)$ ,  $W$  is the pixel width of rail. The green vertical line in Figure 3 is the extracted rail edge.

### 3.2 ASW (Adjusted Sliding Window) Algorithm

The size of the bolt area is  $370 \times 430$  pixels, and the longitudinal distance of the bolt is about 1540 pixels. Thus, the size of the sliding window was set as  $370 \times 430$  pixels, and the subgraph was extracted with a stride length of 1350 pixels and a small step length of 2 pixels. The process of sliding window is shown in figure 4.

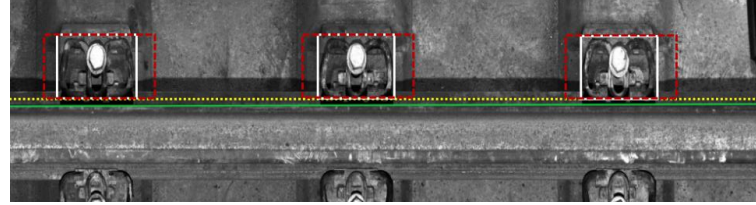


Figure 4: Process of sliding window algorithm. The white boxes are exact location for bolts. The red dotted boxes were calculated by the location of the previous bolt and the gap. The Horizontal green dotted line is the edge of the rail detected in previous step

For each area taken by sliding window, we use structural similarity measurement to measure the difference between it and the template. Calculating method is formula (2).

$$SSIM(X, Y) = \frac{(2u_X u_Y + C_1)(2\sigma_{XY} + C_2)}{(u_X^2 + u_Y^2 + C_1)(\sigma_X^2 + \sigma_Y^2 + C_2)} \quad (2)$$

Where,  $u_X$  and  $u_Y$  respectively represent the mean values of coupler images X and Y,  $\sigma_X$  and  $\sigma_Y$  respectively represent the standard deviations of coupler images X and Y.  $\sigma_{XY}$  represent the covariance of coupler images X and Y, which are usually constant. The value of SSIM is between [0,1]. The larger the value is, the more similar the two images are.

## 4. Bolt Defect Algorithm Based on Bidirectional Generative Adversarial Network

### 4.1 Dataset

We use RSD algorithm and ASW algorithm to process 10000+ railway pictures, then extract 17000+ bolt subgraphs. We manually labeled these bolt subgraphs. Figure 5 shows some extracted bolt subgraphs.



(a)



(b)

(a) shows defective ones; (b) shows defect-free ones.

Figure 5: Some extracted bolt subgraphs.

### 4.2 Bidirectional Generative Adversarial Network (BiGAN)

Bidirectional Generative Adversarial Networks (BiGANs) (Figure 6) was proposed by Jeff Donahue[11] in 2017. Its structure is based on Variational auto-encoder (VAE) and traditional adversarial generation network GAN[12]. It is composed of Generator (G), discriminator (Discriminator, D) and Encoder (E).

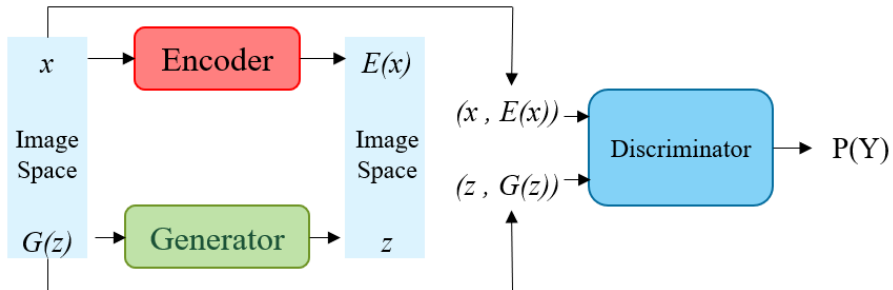


Figure 6: The structure of Bidirectional Generative Adversarial Networks (BiGAN).

The generator G accepts random noise and generates images, while D accepts paired data from

image space and feature space and generates the probability that the input is a real image. The network model constructed in this work is shown in Table 1 and 2.

Table 1: The detailed specifications of G

| Layer | Type               | Kernel       | Depth    | Stride       |
|-------|--------------------|--------------|----------|--------------|
| Input | -                  | -            | 128      | -            |
| 1     | FC                 | $5 \times 5$ | 8192/128 | $2 \times 2$ |
| 2     | Deconv+B<br>N+ReLU | $5 \times 5$ | 256      | $2 \times 2$ |
| 3     | Deconv+B<br>N+ReLU | $5 \times 5$ | 128      | $2 \times 2$ |
| 4     | Deconv+B<br>N+ReLU | $5 \times 5$ | 64       | $2 \times 2$ |

Table 2: The detailed specifications of D/E

| Layer | Type          | Kernel       | Depth    | Stride       |
|-------|---------------|--------------|----------|--------------|
| Input | -             | -            | 64       | -            |
| 1     | Conv+R<br>eLU | $5 \times 5$ | 64       | $2 \times 2$ |
| 2     | Conv+BN+ReLU  | $5 \times 5$ | 128      | $2 \times 2$ |
| 3     | Conv+BN+ReLU  | $5 \times 5$ | 256      | $2 \times 2$ |
| 4     | Conv+BN+ReLU  | $5 \times 5$ | 512      | $2 \times 2$ |
| 5     | FC            | -            | 8192/128 | -            |

FC: fully connected; BN: batch normalizing; ReLU: rectified linear unit.

The network training strategy used in this work is to first use the normal sample training generator and discriminator, which is consistent with the traditional GAN training method. Then, the trained generator is used to train the encoder, and finally all the three structures have good effects. The specific training steps are shown in Figure 7. The training results are shown in Figure 8.

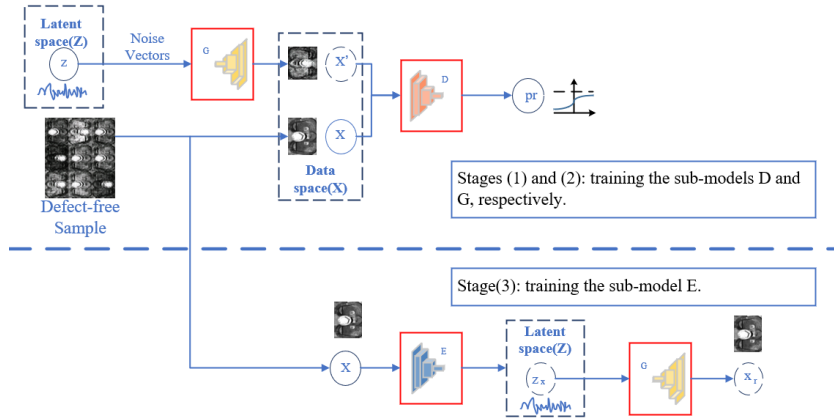


Figure 7: Bolt detection framework: training process.

#### 4.3 Parameter Calibration

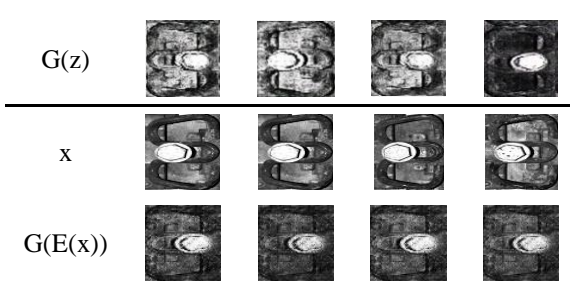


Figure 8: Qualitative results for defect-free datasets BiGAN training, including generator samples  $G(z)$ , real data  $x$ , and corresponding reconstructions  $G(E(x))$ .

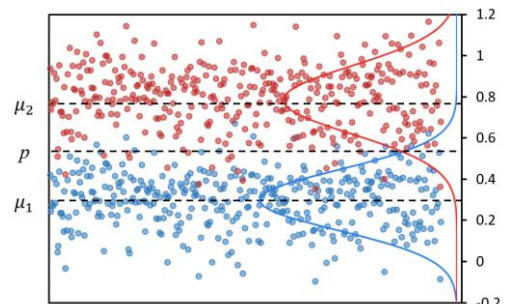


Figure 9: Result analysis: the blue and red spots are results of defect and defect-free blots respectively, the blue and red lines are approximate normal distribution curves for defect and defect-free blots respectively.

The BiGAN discriminator output value is close to 1 for real images and close to 0 for fake images. The normal samples and defect samples were input into the discriminator, and the two groups of data

were tested for hypothesis. The normal samples approximated to  $N(0.8031, 0.0171)$ , while the defective samples approximated to  $N(0.0301, 0.0148)$ . Considering that the discriminator should make the detection rate of defective samples as high as possible, the threshold is set as 0.587. That is, when  $P(Y) < 0.587$ , considers the input image to be a normal sample, and when  $P(Y) > 0.587$ , considers the input image to be a defective sample.

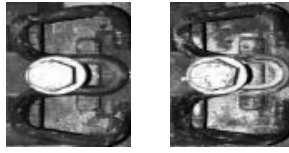
## 5. Experiments and Analysis

The network has a good discriminant effect on the condition of missing boltboard, stampings and loose displacement of boltboard, but it cannot be completely detected when the boltboard has slight deformation. The total recall rate and misjudgment rate are 93.45% and 5.13%, respectively, which are significantly improved compared with the recall rate of about 80% and misjudgment rate of about 10% of existing methods.

Table 3: The result of discriminator.

|                  | Defective sample detection rate | Missing              | Accuracy             | Normal sample misjudgment rate |
|------------------|---------------------------------|----------------------|----------------------|--------------------------------|
| Previous methods | 80% <sup>[4]</sup>              | 85.8% <sup>[5]</sup> | 55.8% <sup>[4]</sup> | -                              |
| Our method       | 93.45%                          | 98.62%               | 94.20%               | 5.13%                          |

The network has a good discriminant effect on the condition of missing springboard, stampings and loose displacement of springboard, but it cannot be completely detected when the springboard has slight deformation. The total recall rate and misjudgment rate are 93.45% and 5.13%, respectively, which are significantly improved compared with the recall rate of about 80% and misjudgment rate of about 10% of existing methods.



(a) (b)

Figure 10: Some undetected defective bolt samples.

## 6. Conclusion

In this work, the structural characteristics of the rail fastener are considered. By using the RSD algorithm and ASW algorithm, the speed of extracting bolt subgraphs can be improved. This work breaks the conventional method of using the existing defect bolt database for identification, and uses the normal sample for network training, identifying the bolts different from the normal ones as the defective bolts. The recognition rate of the wrong sample in this work reached 93.45%, and the misjudgment rate of the correct sample was 5.13%. By preprocessing the images and improving the network structure, the recognition rate is expected to increase to 98.00% and be applied to practical engineering environment.

## References

- [1] Liu Junbo, Huang Yaping, Wang Shengchun, Zhao Xinxin, Zou Qi, Zhang Xingyuan. Defect detection method of multi-track rail bolts based on machine vision [J]. China railway science,2019, 40(04):27-35.
- [2] Fan Hong, Hou Yun, Li Bolin, XIONG Ying. Adaptive vision detection algorithm for bolts of high-speed railway [J]. Journal of southwest jiaotong university, 2020,55(04):896-902.
- [3] Lin Fei, Yang Ziming, Li Yongguang, Wu Kuan, Cui Tingrui. Research on Detection Technology

of Rail Bolts [J]. China Railway,2019(06):103-110.

- [4] Dai Peng, Wang Shengchun, Du Xinyu, Han Qiang, Wang Hao, Ren Shengwei. Image recognition method of ballastless track bolt defects based on semi-supervised deep learning [J]. China railway science,2018, 39(04):43-49.
- [5] Min Yongzhi, XIAO Benyu, Dang Jianwu, et al. Machine Vision Rapid Detection Method of the Track Fasteners Missing[J]. Journal of Shanghai Jiaotong university, 2017,51(10): 1268-1272.
- [6] Tao Xian, Hou Wei, Xu De. A Review of Surface Defect Detection Methods Based on Deep Learning [J]. Acta Automatica Sinica, 2021,47(05): 1017-1034.
- [7] Hu G H, Huang J F, Wang Q H, Li J R, Xu Z J, Huang X B. Unsupervised fabric defect detection based on a deep convolutional generative adversarial network. Textile Research Journal, 2020, 90(3-4): 247–270 doi: 10.1177/0040517519862880
- [8] HUANG Y, LUO S, WANG S. Combining Boundary and Region Information with Bolt Prior for Rail Surface Detection[J]. IEICE Transactions on Information and Systems, 2012,E95-D(2): 690-693.
- [9] Gioi R G V, Jakubowicz J, Morel J M, et al. LSD: A Fast Line Segment Detector with a False Detection Control[J]. IEEE Trans Pattern Anal Mach Intell, 2010, 32(4):722-732.
- [10] Zhou W, Bovik A C, Sheikh H R, et al. Image quality assessment: from error visibility to structural similarity[J]. IEEE Trans Image Process, 2004, 13(4).
- [11] Jeff Donahue, Trevor Darrell (2017.4). Adversarial feature learning. UCB-ICLR2017.
- [12] Goodfellow I J, Pouget-Abadie J, Mirza M, et al. Generative Adversarial Networks[J]. Advances in Neural Information Processing Systems, 2014, 3:2672-2680.